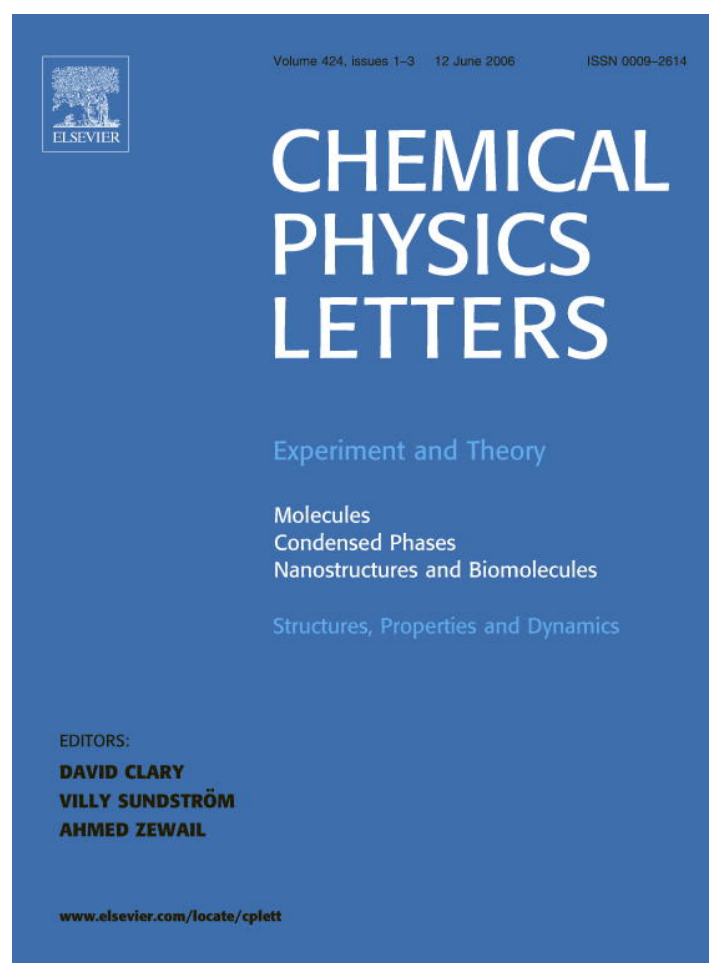


Provided for non-commercial research and educational use only.
Not for reproduction or distribution or commercial use.



This article was originally published in a journal published by Elsevier, and the attached copy is provided by Elsevier for the author's benefit and for the benefit of the author's institution, for non-commercial research and educational use including without limitation use in instruction at your institution, sending it to specific colleagues that you know, and providing a copy to your institution's administrator.

All other uses, reproduction and distribution, including without limitation commercial reprints, selling or licensing copies or access, or posting on open internet sites, your personal or institution's website or repository, are prohibited. For exceptions, permission may be sought for such use through Elsevier's permissions site at:

<http://www.elsevier.com/locate/permissionusematerial>

Photoluminescence of CdSe/ZnS core/shell quantum dots enhanced by energy transfer from a phosphorescent donor

P.O. Anikeeva^{a,*}, C.F. Madigan^a, S.A. Coe-Sullivan^a, J.S. Steckel^b,
M.G. Bawendi^b, V. Bulović^a

^a *Laboratory of Organic Optics and Electronics, Department of Electrical Engineering and Computer Science, Massachusetts Institute of Technology, Cambridge, MA 02139, USA*

^b *Department of Chemistry, Massachusetts Institute of Technology, Cambridge, MA 02139, USA*

Received 11 February 2006; in final form 3 April 2006

Available online 21 April 2006

Abstract

We demonstrate exciton energy transfer from a thin film of phosphorescent dye *fac* tris(2-phenylpyridine) iridium ($\text{Ir}(\text{ppy})_3$) to a monolayer of colloidal CdSe/ZnS core/shell quantum dots (QDs). The energy transfer is manifested in time-resolved photoluminescence (PL) measurements as elongation of the QD PL time constant from 40 to 400 ns, and a concomitant 55% increase of time-integrated QD PL intensity. The observed PL dynamics are shown to be dominated by exciton diffusion within the $\text{Ir}(\text{ppy})_3$ film to the QD layer.
© 2006 Elsevier B.V. All rights reserved.

Over the past several years the optical and electronic properties of colloidal synthesized nanocrystals [1], or quantum dots (QDs), of CdSe have been extensively studied with the aim of using QD films in solid state opto-electronic devices. Efficient exciton generation in CdSe QDs suggests use of nanocrystal composite films in photovoltaic cells [2], while high luminescence quantum yields and tunability of QD emission wavelengths over the entire visible spectrum suggests QD film use in light emitting devices (LEDs) [3]. These developments are a consequence of advances in colloidal QD synthesis that allow for increased control over the shape, size, and emission wavelength of nanocrystals [4], and the development of methods for forming QD thin films of controlled structure and composition [5]. Utilizing these advances, in the present Letter we fabricate hybrid organic thin film/QD structures which demonstrate triplet exciton energy transfer (ET) from a thin film of phosphorescent molecules to a monolayer of CdSe/ZnS core/shell QDs. Triplet exciton harvesting and transfer to an efficient lumino-

phore has been previously used in advancing organic light emitting device (OLED) technology [6], and has the potential to similarly benefit the emerging field of quantum-dot-LEDs (QD-LEDs) [7].

OLEDs based on phosphorescent materials exhibit high quantum efficiencies [8]. For example, organic phosphors containing d^6 Ir^{3+} complexes, such as the *fac* tris(2-phenylpyridine) iridium ($\text{Ir}(\text{ppy})_3$) that is used in this Letter (see inset of Fig. 1) [9,10], show record efficient electro-phosphorescence at room temperature with external quantum efficiencies as high as 19% [11]. In these compounds spin-orbit coupling leads to the mixing of the spin-singlet and spin-triplet excited states [10,12], which enables the radiative relaxation of the triplet-state and leads to a fast phosphorescent decay ($<1 \mu\text{s}$) and high phosphorescence efficiency that benefits OLED performance.

In QDs, the presence of transition metal atoms, such as Cd, leads to electron-hole exchange interaction and spin-orbit coupling [13] that mix the electron and hole spin states. In CdSe QDs electron spin-mixing results in a non-emissive lowest energy exciton, so called 'dark exciton' [14], which is between 0.13 meV (as in CdSe bulk) and 12.5 meV (for the smallest QD with few nm diameter)

* Corresponding author.

E-mail address: anikeeva@mit.edu (P.O. Anikeeva).

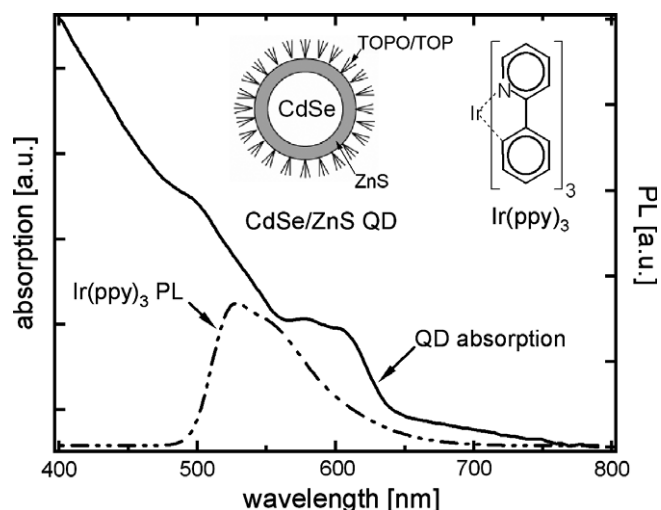


Fig. 1. Overlap between CdSe/ZnS QD absorption (solid line) and Ir(ppy)₃ emission (dash-dot-dot) spectra suggests energy transfer from Ir(ppy)₃ to QDs. (Note. QD absorption spectrum was obtained by the direct measurement in a thin film, consequently it exhibits a red tail due to the scattering of the organic ligands in a solid film.) Inset: Schematic drawing of a ZnS overcoated CdSe QD and Ir(ppy)₃ structural formula.

below the emissive excitonic state [15]. Thermal mixing of the dark and emissive exciton results in a room temperature QD radiative lifetime in the range from 3 to 30 ns (depending on the QD core/shell structure, size distribution, and the fidelity of the organic capping layer), and luminescence efficiencies exceeding 80% in solution [16,17].

Since QDs are efficient lumophores and Ir(ppy)₃ is an efficient triplet exciton harvester, in this Letter we consider energy transfer (ET) from Ir(ppy)₃ to CdSe/ZnS core/shell QDs in order to enhance the luminescence intensity of QD lumophores. Overlap of Ir(ppy)₃ luminescence and QD absorption spectra suggests the possibility of efficient ET (Fig. 1). Our Letter follows earlier experiments that investigated Förster ET to CdSe/ZnS QDs from both fluorescent organic hosts as well as from inorganic substrate layers [18,19]. QDs have proven themselves as efficient exciton donors in energy transfer experiments with various organic dyes and bioorganic molecules [20,21]; however, there remains debate in the literature over the demonstration of ET from an organic donor to CdSe/ZnS core/shell QD (see e.g. [22]). In contrast, the present Letter definitively confirms that CdSe/ZnS core/shell QDs can efficiently accept excitons from an organic donor by demonstrating ET of triplet excitons from a phosphorescent dye to QD lumophores.

We fabricated three thin film structures: sample I is a 40 nm thick film of 10% Ir(ppy)₃ doped into 4,4'-N,N'-dicarbazole-biphenyl (CBP) thermally evaporated onto a glass substrate. Sample II is a monolayer of CdSe/ZnS QDs (7 nm QD diameter) printed [23] onto a glass substrate. Finally, sample III is a hybrid structure consisting of a monolayer of CdSe/ZnS QDs printed onto a 40 nm thick film of 10% Ir(ppy)₃ in CBP on glass.

Comparing the PL signatures of the three samples we observe a $21 \pm 4\%$ decrease of Ir(ppy)₃ time-integrated PL intensity in sample III as compared to sample I and a concomitant $55 \pm 5\%$ increase in CdSe/ZnS QD film PL intensity in sample III as compared to sample II (see Fig. 2). The change in PL is calculated by numerically decomposing the sample III spectrum into CdSe/ZnS QD and Ir(ppy)₃ components. The PL change suggests ET from the Ir(ppy)₃ film to the QD monolayer. We note that simple reabsorption of Ir(ppy)₃ luminescence by the QD film does not account for the observed PL change since the 7 nm thick QD monolayer has very weak absorption ($<1.5\%$) over the Ir(ppy)₃ PL spectrum. Assuming a QD PL efficiency on the order of 0.1 (typical of QD films), we find that reabsorption of Ir(ppy)₃ photons by the QD layer can lead to small QD PL flux increase of at most 0.0015 times the Ir(ppy)₃ photon flux, or a roughly three orders of magnitude smaller than the observed QD intensity. (To provide an upper limit on the reabsorption effect, we assume all of the Ir(ppy)₃ flux is directed through the QD film.) Consequently, reabsorption does not significantly contribute to the observed increase in QD PL in sample III. (Note that because the film thicknesses are much less than the wavelengths of the emitted light, and the refractive index contrasts between the layers are small, optical cavity effects are not expected to be significant.)

Data from time-resolved PL measurements are shown in Fig. 3. The PL of CdSe/ZnS QDs in sample II (data set E) exhibits two time constants with a shorter time constant of $\tau_1^{\text{QD}} = 10$ ns and a longer time constant of $\tau_2^{\text{QD}} = 40$ ns. The Ir(ppy)₃ PL decay also exhibits bi-exponential behavior, with a dominant time constant of $\tau^{\text{Ir(ppy)}_3} = 610$ ns (as obtained from data set A). In sample III, however, the QD PL decay (data set D) is substantially elongated, leading to a longer time constant of $\tau_{2,\text{III}}^{\text{QD}} = 500$ ns, which is

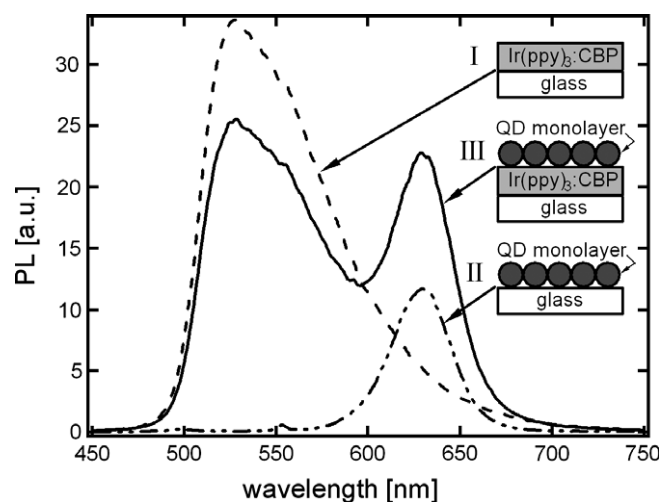


Fig. 2. Time-integrated PL spectra of samples I, II and III. All measurements were obtained at the same excitation source power of $\lambda = 395$ nm light. The PL spectrum of sample III can be constructed from a linear superposition of the PL spectra of samples I and II.

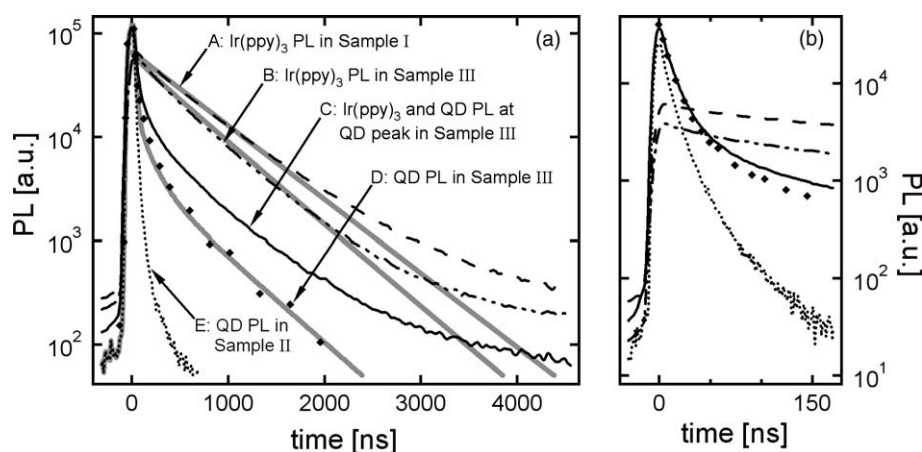


Fig. 3. Time resolved PL measurements for samples I, II and III, performed over (a) a 5000 ns time window and (b) a 500 ns time window (first 200 ns shown). The black lines and dots represent the experimental measurements, and the thick grey lines represent numerical fits using the proposed diffusion model. To obtain data sets A and B, the sample PL was integrated over the wavelength range of $\lambda = 511$ nm to $\lambda = 568$ nm, to yield in each case the time dependence of the Ir(ppy)₃ PL. Similarly, to obtain data sets C and E, a wavelength range of $\lambda = 600$ nm to $\lambda = 656$ nm was used. Data set C therefore reflects the intensity of combined Ir(ppy)₃/QD PL near the QD PL peak. Data set E reflects the intensity of solely the QD PL. To obtain data set D, the intensity due to the Ir(ppy)₃ PL was subtracted from C to yield just the QD PL intensity in sample III. Note that the grey fit lines assume a single exponential time decay for the Ir(ppy)₃, and so are only expected to fit the Ir(ppy)₃ at early times (where the single exponential decay dominates).

identical to the dominant time constant of the Ir(ppy)₃ PL from the same sample (data set B), strongly suggesting that this ‘delayed’ QD PL is due to energy transfer of Ir(ppy)₃ excitons to the QD film.

An investigation of the first 200 ns of QD PL (Fig. 3b) reveals a slight increase in the initial PL intensity and a small increase of the short time constant, yielding $\tau_{1,sIII}^{QD} = 12$ ns. Note that in Fig. 3, the data are obtained by integrating the PL spectra over the wavelength ranges specified in the figure caption. Furthermore, the QD PL decay for sample III (data set D) is obtained by subtracting the Ir(ppy)₃ PL spectrum from the total signal, as illustrated in Fig. 4, and then integrating the difference signal over the specified wavelength range. We again note that the time-dependent contribution of reabsorption to the

QD PL is at most 0.0015 times the Ir(ppy)₃ flux intensity (obtained from sample I). Therefore, for all times reabsorption contribution is at most 3% of the observed QD PL signal.

Since reabsorption does not contribute significantly to the QD PL intensity in sample III, the observed QD PL enhancement and elongation of QD PL lifetime can be attributed to exciton energy transfer from Ir(ppy)₃ molecules to the QD monolayer. For quantitative analysis of the data, we note that the observed PL time dependence (Figs. 3 and 4) is shaped by four physical processes that govern exciton dynamics in the Ir(ppy)₃:CBP film: Ir(ppy)₃ exciton radiative decay, non-radiative decay, ET to the QD film, and diffusion. The two decay mechanisms combine to determine the observed radiative lifetime of 610 ns and a

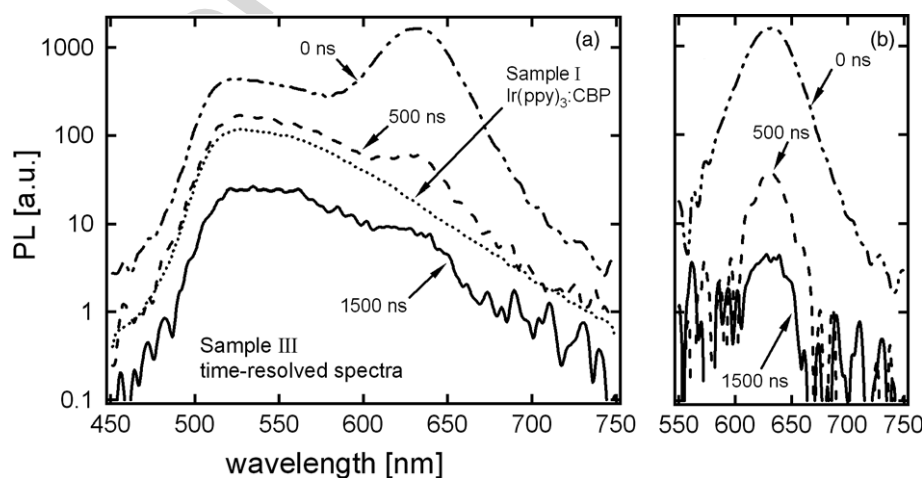


Fig. 4. (a) PL spectra of sample III are shown at times $t = 0$ ns (dash-dot-dot), $t = 500$ ns (dashed line), $t = 1500$ ns (solid line) after excitation. Ir(ppy)₃ integrated PL spectrum (dotted line) is shown for comparison (not to scale). (b) QD PL in sample III obtained by subtracting scaled Ir(ppy)₃ spectrum from the PL of sample III is shown at $t = 0$ ns (dash-dot-dot), $t = 500$ ns (dashed), $t = 1500$ ns (solid) after excitation.

PL quantum efficiency of $\sim 15\%$ (as calculated from optimized electroluminescence efficiencies of 12% doped Ir(ppy)₃:CBP OLEDs [24]). The ET mechanism leads to the observed quenching of the Ir(ppy)₃ PL and the associated enhancement of the QD PL, and capturing the Ir(ppy)₃ excitons that are closest to the QD film. Finally, the diffusion mechanism induces a net flow of Ir(ppy)₃ excitons towards the QD film, due to depletion by ET of Ir(ppy)₃ excitons near the QD interface.

To numerically model the combined processes we model the ET mechanism as an instant energy transfer of any Ir(ppy)₃ exciton that is within distance, L_{ET} , from the QD film. In this model the dynamics of the ET process is controlled entirely by Ir(ppy)₃ exciton diffusion, which determines the rate at which excitons are supplied to the region within L_{ET} of the QD film.

A reasonable value for L_{ET} is determined by considering the possible ET mechanisms. In the case of ET by correlated electron exchange, a mechanism also known as Dexter transfer [25], the exciton capture region consists of a single Ir(ppy)₃ layer adjacent to QDs, since the transfer rate falls off exponentially with distance, reducing to negligible the ET contributions from all the more distant molecular layers. Since the Ir(ppy)₃ molecule is on the order of 1 nm in extent, then we estimate that $L_{ET} = 1$ nm for Dexter energy transfer.

In the case of resonant ET, a mechanism also known as Förster transfer, the capture region can be larger. For Förster transfer, the rate of ET between a donor (D) and an acceptor (A), is given by [26]

$$K_{D \rightarrow A} = \frac{1}{\tau} \left(\frac{R_F}{R} \right)^6 \quad (1)$$

where R is the distance between the donor and the acceptor, τ is the donor lifetime, and, R_F is a Förster radius

$$R_F^6 \equiv \frac{9}{8\pi} \frac{c^4}{n^4} \kappa^2 \eta_D \int \frac{S_D(\omega) \sigma_A(\omega)}{\omega^4} d\omega \quad (2)$$

where c is the speed of light in vacuum, n is the index of refraction of the medium, κ is an orientational factor, η_D is the donor PL quantum efficiency, S_D is the donor emission spectrum (normalized to integrate over frequency to unity), and σ_A is the acceptor absorption cross-section.

We calculate $R_F = 4.1$ nm from (2) by inserting the donor Ir(ppy)₃ PL and acceptor QD absorption spectra shown in Fig. 1, setting $n = 1.7$ and $\kappa^2 = 2/3$ (which averages the result over randomly oriented donor and acceptor dipoles), and using $\eta_D = 0.15$ (as estimated above). (Note. We use $n = 1.7$ characteristic of organic thin films to obtain an upper bound on R_F . Locally the refractive index could be higher due to the higher QD index, of $n \sim 2.1$, which would lead to a lower R_F value.) This R_F value is roughly equal to the center-to-center distance between a QD and an adjacent Ir(ppy)₃ molecule, i.e. 3.5 nm (half the QD diameter) + 0.5 nm (half the extent of the Ir(ppy)₃ molecule) = 4.0 nm. We, therefore, expect that Ir(ppy)₃-to-QD Förster ET is dominated by nearest neighbor trans-

fers. However, it is worth noting that the total rate of energy transfer from a single organic molecule to a QD layer should be integrated over all of the dots in the QD layer. This calculation yields a total transfer rate that scales as R^{-4} [27]. For a hexagonally close packed QD monolayer, the total rate is given by

$$K_{D-AL} = \frac{1}{\tau} \frac{R_F^6}{2a^2 R^4} = \frac{1}{\tau} \frac{D_F^4}{R^4} \quad (3)$$

where a is the radius of the QD. Using the values for a and R_F , we obtain $D_F = 3.7$ nm.

Given that as noted above the transfer distance between nearest neighbors is just 4.0 nm, we conclude, as expected from the R_F calculation, that transfer is dominated by the layer of donors in immediate contact with the QD layer, and thus we set $L_{ET} = 1$ nm. (We note that reabsorption, Förster, and Dexter are the most commonly proposed ET mechanisms and are, hence, the mechanisms focused on in this Letter. The following analysis, however, is unchanged even for other ET mechanisms, so long as L_{ET} remains of the order of 1 nm.)

We model the emission, diffusion, and ET processes in Ir(ppy)₃ through a differential equation governing the time, t , and space, x , dependence of the exciton population, $n(x, t)$, in the Ir(ppy)₃ film:

$$\frac{d}{dt} n(x) = -\frac{1}{\tau} \left(-n(x) + L_D^2 \frac{d^2}{dx^2} n(x) \right), \quad 0 \leq x < L - L_{ET} \quad (4)$$

where L is the total thickness of the Ir(ppy)₃ film and $x = L$ is the Ir(ppy)₃/QD interface. For the film region comprising $x \geq L - L_{ET}$, we assume that any non-zero value of n is instantly lost due to ET to QD film. We further assume that initially, at $t = 0^-$, the film is uniformly excited and a moment later, at $t = 0^+$, for $x \geq L - L_{ET}$, all of the exciton concentration is lost to ET. (Because the film absorbs less than 20% of the incident excitation light, the error incurred in assuming uniform excitation is small.) Subsequently, the system evolves following Eq. (4) with diffusion current through the $x = L - L_{ET}$ plane comprising the Ir(ppy)₃ excitons lost to ET due to diffusion. We perform a discrete time numerical calculation of two functions of this system: the number of emitted photons per time step, $n_{PL}(t)$, and the number of energy transferred excitons per time step, $n_{ET}(t)$. Setting $L = 40$ nm, $L_{ET} = 1.0$ nm and $\tau = 610$ ns we find that for a 21% Ir(ppy)₃ quenching fraction, we obtain $L_D = 8.1$ nm. In Fig. 3 we plot the associated fits (grey lines). The $n_{PL}(t)$ function provides the fit to the Ir(ppy)₃ PL in sample III. To fit the QD PL in sample III, we scale the $n_{ET}(t)$ function by 0.6 relative to the Ir(ppy)₃ PL curve (to reflect the reduced PL efficiency of QDs as compared to Ir(ppy)₃ and the spectral collection window) and add to it the QD PL observed in sample II, which provides the PL due to direct excitation of the QD film. For comparison, a single exponential decay with $\tau = 610$ ns is plotted besides Ir(ppy)₃ PL of sample I (data set A).

The model generated PL time dependence is consistent with both the Ir(ppy)₃ and QD time dependent PL intensity from sample III. For the Ir(ppy)₃ PL (data set B), the deviations mainly occur at longer times ($t > 2000$ ns) where the single exponential character of the intrinsic Ir(ppy)₃ PL is no longer valid. For the QD PL (data set D), the fit agrees to within the experimental error at all times. The fit suggests that the QD PL is initially due to both PL of QDs excited by incident light and PL of QDs excited by ET from Ir(ppy)₃. At later times ($t > 150$ ns) the QD PL dynamics are due entirely to the Ir(ppy)₃ exciton diffusion process. We also note that the value of $L_D = 8.1$ nm obtained from the fit is comparable to exciton L_D values measured in other molecular organic thin film systems [28,29].

By considering the scaling factor required to fit the QD PL in sample III (data set D) we can calculate the PL efficiency of the QD film. Due to the measurement windows utilized in generating the intensity profiles in Fig. 3, the Ir(ppy)₃ PL curve (comprising the signal between $\lambda = 511$ nm and $\lambda = 568$ nm) reflects 0.59 of the total Ir(ppy)₃ spectral intensity, while the QD PL curve (comprising the signal between $\lambda = 600$ nm and $\lambda = 656$ nm) reflects 0.86 of the total QD spectral intensity. Consequently, transferring Ir(ppy)₃ excitons to the QD layer should yield a corresponding increase in QD PL curve equal to $0.86/0.59 = 1.46$ times the loss in Ir(ppy)₃ photons for equal quantum efficiencies. Since we fit our QD PL data by scaling the $n_{ET}(t)$ curve down by 0.6 relative to the Ir(ppy)₃ fit, this implies the quantum efficiency, η_{QD} , of the QD film is $0.6/1.46 = 0.41$ times the Ir(ppy)₃ quantum efficiency, yielding $\eta_{QD} = 0.41 \times 0.15 = 0.06$, which is consistent with typical thin film QD PL efficiencies.

Finally, we note that the model employed here is only weakly dependent on L_{ET} , with the main effect being that as L_{ET} increases, L_D decreases because a larger fraction of the Ir(ppy)₃ photons are instantly quenched and therefore less diffusion is required to obtain the desired 21% total quench. In the rather extreme case where $L_{ET} = 5$ nm, the data can still be roughly fit by setting $L_D = 4.0$ nm, yielding a corresponding calculation of $\eta_{QD} = 0.12$. Indeed, we find that this model produces a similar time dependence to the Ir(ppy)₃ PL quench and QD PL enhancement for a wide range of L_{ET} values. Consequently, on the basis of only the experiments shown here, it is not possible to conclusively identify the dominant ET mechanism (e.g., Dexter or Förster).

In conclusion, we report an increase in the PL intensity and an increase in PL lifetime for a CdSe/ZnS QD thin film due to exciton ET from a phosphorescent molecular organic film. The observed ET dynamics are self-consistently explained by a simple numerical model that combines exciton diffusion in the Ir(ppy)₃ film with short-range ET from Ir(ppy)₃ to the QD layer. The demonstrated transfer of triplet excitons to luminescent QDs could benefit the development of QD optoelectronic technologies, such as QD-LEDs.

1. Experimental

Thermal deposition of the organic films was performed at a rate of ~ 0.2 nm/s and a chamber pressure of $< 2 \times 10^{-6}$ Torr. CdSe/ZnS QDs were prepared using a procedure similar to that described in [4]. Prior to the thin film deposition the glass substrates were cleaned by a multiple step solvent cleaning process using Micro 90, acetone and isopropanol. To prevent exposure to an ambient environment during measurements, samples were packaged inside a nitrogen glovebox using a glass coverslip and UV-curing epoxy.

In the time resolved photoluminescence measurement the excitation source was $\lambda = 395$ nm wavelength laser light with 200 fs pulse width and 100 kHz repetition rate obtained by frequency doubling the output of a Coherent Ti-Sapphire laser. Photoluminescence was collected with a Hamamatsu C4780 picosecond fluorescence lifetime system consisting of a C4334 streak camera and a C5094 spectrograph. The light collection scheme consisted of two lenses, one collecting luminescence from a sample and the other focusing it onto a detector slit. Laser beam was incident on the sample at approximately 60° angle away from the normal, and the collecting lens was aligned normal to the sample. All three samples were excited with a constant laser power of 33 mW/cm² without altering the collection geometry, allowing a relative comparison of PL intensities. All measurements were performed at room temperature.

Acknowledgements

The authors are grateful for financial support of the MIT Institute for Soldier Nanotechnologies, NSF Materials Research Science and Engineering Center at MIT, and the Presidential Early Career Award for Scientists and Engineers. PA would like to thank Steven E. Kooi for his assistance with time-resolved PL measurements.

References

- [1] C.B. Murray, D.J. Norris, M. Bawendi, J. Am. Chem. Soc. 115 (1993) 8706.
- [2] W.U. Huynh, J.J. Dittmer, A.P. Alivisatos, Science 295 (2002) 2425.
- [3] S. Coe, W.-K. Woo, M.G. Bawendi, V. Bulovic, Nature (London) 420 (2002) 800.
- [4] B.O. Dabbousi, J. Rodriguez Viejo, F.V. Miculec, J.R. Heine, H. Mattoussi, R. Ober, K.F. Jensen, M.G. Bawendi, J. Phys. Chem. B 101 (1997) 9463.
- [5] S. Coe-Sullivan, J.S. Steckel, W.-K. Woo, M.G. Bawendi, V. Bulovic, Adv. Funct. Mater. 15 (2005) 1117.
- [6] M.A. Baldo, M.E. Thompson, S.R. Forrest, Nature (London) 403 (2000) 750.
- [7] S. Coe-Sullivan, J.S. Steckel, L. Kim, M.G. Bawendi, V. Bulovic, Proc. SPIE 5739 (2005) 108.
- [8] M.A. Baldo, D.F. O'Brien, M.E. Thompson, S.R. Forrest, Phys. Rev. B 60 (1999) 14422.
- [9] K. Dedeian, P.I. Djurovich, F.O. Garces, G. Carlson, R.J. Watts, Inorg. Chem. 30 (1991) 1685.

- [10] S. Lamansky, P. Durovich, D. Murphy, F. Abdel-Razzaq, H.-E. Lee, C. Adachi, P.E. Burrows, S.R. Forrest, M. Thompson, *J. Am. Chem. Soc.* 123 (2001) 4304.
- [11] C. Adachi, M.A. Baldo, M.E. Thompson, S.R. Forrest, *J. Appl. Phys.* 90 (2001) 5048.
- [12] M.A. Baldo, D.F. O'Brien, Y. You, A. Shoustikov, S. Sibley, M.E. Thompson, S.R. Forrest, *Nature (London)* 395 (1998) 151.
- [13] P.W. Atkins, R.S. Friedman, *Molecular Quantum Mechanics*, Oxford University Press, Oxford, 1997.
- [14] M. Nirmal, D.J. Norris, M. Kuno, M.G. Bawendi, A.L. Efros, M. Rosen, *Phys. Rev. Lett.* 75 (1995) 3728.
- [15] A.L. Efros, M. Rosen, *Annu. Rev. Mater. Sci.* 30 (2000) 475.
- [16] M.A. Hines, P. Guyot-Sionnest, *J. Phys. Chem.* 100 (1996) 468.
- [17] P. Reiss, J. Bleuse, A. Pron, *Nano Lett.* 2 (2002) 781.
- [18] M. Anni, L. Manna, R. Cingolani, D. Valerini, A. Creti, M. Lomascolo, *Appl. Phys. Lett.* 85 (2004) 4169.
- [19] M. Achermann, M.A. Petruska, S. Kos, D.L. Smith, D.D. Koleske, V.I. Klimov, *Nature (London)* 429 (2004) 642.
- [20] A.R. Clapp, I.L. Medintz, J.M. Mauro, B.R. Fisher, M.G. Bawendi, H. Mattoussi, *J. Am. Chem. Soc.* 126 (2004) 301.
- [21] I.L. Medintz, A.R. Clapp, H. Mattoussi, E.R. Goldman, B.M. Fisher, J.M. Mauro, *Nat. Mater.* 2 (2003) 630.
- [22] A.R. Clapp, I.L. Medintz, B.R. Fisher, G.P. Anderson, H. Mattoussi, *J. Am. Chem. Soc.* 127 (2005) 1242.
- [23] S. Coe-Sullivan, PhD Thesis, Department of Electrical Engineering and Computer Science, Massachusetts Institute of Technology, 2005.
- [24] M.A. Baldo, S. Lamansky, P.E. Burrows, M.E. Thompson, S.R. Forrest, *Appl. Phys. Lett.* 75 (1999) 4.
- [25] M. Pope, C.E. Swenberg, *Electronic Processes in Organic Crystals*, Oxford University Press, Oxford, 1982.
- [26] Th. Förster, *Annalen der Physik* 6 (1948) 55.
- [27] H. Kuhn, *J. Chem. Phys.* 53 (1) (1970) 101.
- [28] E.B. Namdas, A. Ruseckas, I.D.W. Samuel, S.-C. Lo, P.L. Burn, *Appl. Phys. Lett.* 86 (2005) 091104.
- [29] N. Matsusue, S. Ikame, Y. Suzuki, H. Naito, *Appl. Phys. Lett.* 97 (2005) 123512.

Author's personal